Spatiotemporal dynamics of androgen signaling underlie sexual differentiation and congenital malformations of the urethra and vagina

Christine E. Larkins[a,1], Ana B. Enriquez[a], and Martin J. Cohn[a,b]

[a]Department of Molecular Genetics and Microbiology, University of Florida Genetics Institute, University of Florida, Gainesville, FL 32610; and [b]Department of Biology, University of Florida, Gainesville, FL 32610

Edited by John J. Eppig, The Jackson Laboratory, Bar Harbor, ME, and approved October 5, 2016 (received for review June 27, 2016)

Disorders of sex development (DSDs) are congenital anomalies that affect sexual differentiation of genitourinary organs and secondary sex characters. A common cause of female genital virilization is congenital adrenal hyperplasia (CAH), in which excess androgen production during development of 46XX females can result in vaginal atresia, masculinization of the urethra, a single urogenital sinus, and clitoral hypertrophy or ambiguous external genitalia. Development of the vagina depends on sexual differentiation of the urogenital sinus ridge, an epithelial thickening that forms where the sex ducts attach to the anterior urethra. In females, the sinus ridge descends posteriorly to allow the vaginal opening to form in the vulva, whereas in males and in females with CAH, androgens inhibit descent of the sinus ridge. The mechanisms that regulate development of the female urethra and vagina are largely unknown. Here we show that the timing and duration of, and the cell population targeted by, androgen signaling determine the position of vaginal attachment to the urethra. Manipulations of androgen signaling in utero reveal a temporal window of development when sinus ridge fate is determined. Cell type-specific genetic deletions of androgen receptor (*Ar*) identify a subpopulation of mesenchymal cells that regulate sinus ridge morphogenesis. These results reveal a common mechanism that coordinates development of the vagina and feminization of the urethra, which may account for development of a single urogenital sinus in females exposed to excessive androgen during a critical period of prenatal development.

vagina | urethra | androgen | mouse | development

Disorders of sex development (DSDs) occur in 1 in 4,500 births and are classified as the chromosomal, gonadal, and/or phenotypic sex of an individual being atypical (1–3). Although these conditions are known to result from genetic and/or hormonal perturbations, the developmental mechanisms underlying the associated genitourinary anomalies are poorly understood. Congenital adrenal hyperplasia (CAH) is a genetic disorder that leads to excess androgen production by the fetal adrenal glands, which can cause 46XX individuals to develop masculinized external genitalia (4, 5). Despite appearing male externally, these genetic females have ovaries and corresponding female internal sex organs, including a vagina, but the vagina is attached to the urethra instead of opening in the vulva. The attachment point of the vagina to the urethra can vary from a proximal confluence near the bladder neck to a distal confluence near the perineum. The molecular and cellular mechanisms that coordinate development of the vagina and urethra to generate a vaginal opening within the vulva are largely unknown (6–9).

The vagina is derived from the Müllerian ducts, which also give rise to the oviducts and uterus. Embryonically, the position where the Müllerian ducts attach to the endodermally derived urogenital sinus, the precursor to the urethra, is characterized by an epithelial thickening called the urogenital sinus ridge (also called vaginal plate or sinovaginal bulb). The sinus ridge is also the site of attachment of the Wolffian ducts, which contribute to the male reproductive tract. Development of the vaginal opening within the vulva depends on a series of morphogenetic events. In female mice, the Wolffian ducts degenerate, and, through an unknown mechanism, the relative position of the urogenital sinus ridge and the attached Müllerian ducts shifts distally along the urethra until reaching the vulva at postnatal day (P)3 (7, 10–13). The urogenital sinus ridge detaches from the urethra by P8, and, at puberty, the sinus ridge opens allowing the Müllerian duct-derived vagina to open in the vulva (8, 14, 15).

The mechanisms that govern translocation of sinus ridge position along the urethra are poorly understood, although studies in humans and rodents have shown that descent of the sinus ridge is inhibited by androgens. In mouse and rat embryos exposed to testosterone, lower doses result in a more distal/posterior attachment of the vagina and urethra, whereas higher doses result in more proximal/anterior attachment near the bladder neck (8, 9, 16, 17). Although these studies have begun to explain the variability of phenotypes found in human DSDs, such as CAH, comparatively little is known about (*i*) the critical period of development when the caudal shift of the sinus ridge is responsive to and can be inhibited by androgen signaling; (*ii*) the locations and types of cells within the urogenital sinus that are targeted by androgen to mediate its effects on sinus ridge position; or (*iii*) the molecular mechanisms by which androgen prevents sinus ridge movement. It has been suggested that the timing of androgen exposure in human females contributes to the position of vaginal attachment to the urethra but this remains untested experimentally (18).

Here we report that prenatal exposure of female mice to androgen when the relative position of the sinus ridge is shifting from the bladder neck to the vulva results in the arrest of sinus ridge movement. The timing and duration of androgen exposure determines the

Significance

Disorders of sex development (DSDs) and some non-DSD human syndromes result in female genitourinary malformations. The mechanisms of genitourinary development are beginning to be understood in males; however, little is known about female lower genitourinary organogenesis. Prenatal exposure to excessive endogenous or exogenous androgens can disrupt sexual differentiation of the female urethra and vagina, but the mechanisms responsible for these malformations are not well understood. This study sheds new light on development of vaginal anomalies in DSDs by (*i*) identifying the critical period of female development when vaginal position and feminization of the urethra is established and (*ii*) showing that this process is controlled by an androgen-responsive subpopulation of mesenchymal cells adjacent to the urogenital sinus.

Author contributions: C.E.L. and M.J.C. designed research; C.E.L. and A.B.E. performed research; C.E.L. and M.J.C. analyzed data; and C.E.L., A.B.E., and M.J.C. wrote the paper.

The authors declare no conflict of interest.

This article is a PNAS Direct Submission.

[1]To whom correspondence should be addressed. Email: christinelarkins@ufl.edu.

This article contains supporting information online at www.pnas.org/lookup/suppl/doi:10.1073/pnas.1610471113/-/DCSupplemental.

site of attachment of the vagina to the urethra; chronic androgen exposure during the developmental window of sensitivity causes proximal attachment of the vagina to the urethra, whereas acute exposures or those that occur before E14.5 do not disrupt formation of a vaginal opening in the vulva. Cell type-specific deletions of androgen receptor (AR) identifies the urogenital sinus mesenchyme as the cell population that mediates the effects of androgen on sinus ridge position. Mosaic analysis of conditional mutants suggests that a subpopulation of mesenchymal cells immediately adjacent to the urethral epithelium could be the primary target of androgen signaling for morphogenesis of the urogenital sinus ridge.

Results

Sexual Differentiation of the Urogenital Sinus Ridge. In females, development of the vaginal opening in the vulva requires the urogenital sinus ridge, which forms just below the bladder and shifts posteriorly along the urethra until it reaches the vulva. To determine when the urogenital sinus ridge position becomes sexually dimorphic, we compared the length of the urogenital sinus from the bladder to the sinus ridge in male and female mouse embryos using the Shh^{GFPcre} and $R26R^{lacZ}$ alleles, which allow visualization of the urogenital sinus epithelium after lacZ staining. At embryonic day (E)14.5, the length of the urethra from the bladder to the sinus ridge (anterior urethral length) was identical in male and female embryos (Fig. 1 *A*, *B*, and *I*). No difference in anterior urethral length was found between males and females until E16.5, when females showed increased length from the bladder to the sinus ridge compared with males (Fig. 1 *C*–*F* and *I*). To control for differences in total urethral length between males and females (and for size variation across individuals), we then determined the relative position of the sinus ridge by examining the absolute length of the urethra from the bladder to the sinus ridge and compared this to total urethral length. Both the relative and the absolute positions of the sinus ridge shift along the urethra in females starting at E16.5, whereas in males, the position of the sinus ridge is maintained near the bladder neck (Fig. 1 *J* and *K*).

At E17.5, the urethrae of males and females were markedly different in length and morphology (Fig. 1 *G*–*I*). The male urethra had an S-shaped bend at the base of the phallus, developed enlarged bulbourethral gland buds at the crus of the glans, and initiated prostate budding near the bladder neck (compare Fig. 1*G* to 1*H*). Although the male urethra had lengthened, the sinus ridge remained at its initial relative position along the urethra, indicating that the urogenital sinus proximal and distal to the sinus ridge were lengthening proportionally (Fig. 1 *I*–*K*). By contrast, female urethral length did not change from E16.5 to E17.5, although the relative position of the sinus ridge had shifted further caudally along the urethra (Fig. 1 *I*–*K*). These results show that the morphogenetic events that position the vaginal opening within the vulva are initiated by E16.5, when sinus ridge position begins to shift, and this co-occurs with sexual differentiation of urethral morphology and length.

Timing and Duration of Androgen Exposure in Utero Determines Sinus Ridge Position and Urethral Morphology. Having identified the temporal window during which the relative position of the sinus ridge begins to shift along the urethra, we next investigated the temporal effects of androgen exposure. Pregnant females were administered 12 mg/kg of methyltestosterone (Me-T) by gavage during three time windows: E12.5–E14.5, just before sinus ridge movement; E14.5–E16.5, at the start of sinus ridge movement; and E16.5–E18.5, just after the relative position of the sinus ridge begins to shift (Fig. 2*A*). Mice from treated and control litters were examined at P28, when the sinus ridge has reached the perineum and the vagina has opened in the vulva. Females from both E14.5–E16.5 and E16.5–E18.5 androgen treatment groups lacked a vaginal opening in the vulva; instead, the vaginal and urethral epithelia were connected to form a single urogenital sinus

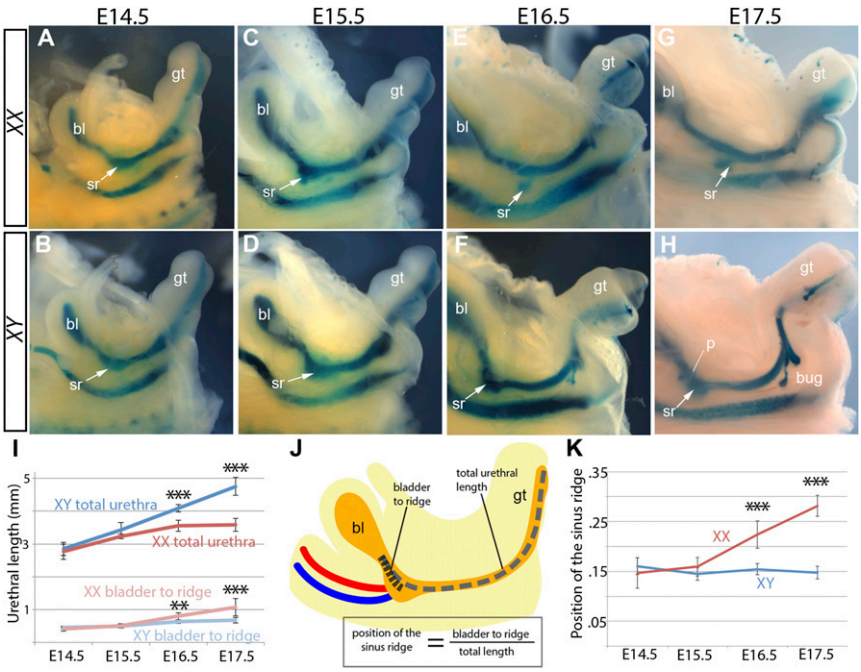

Fig. 1. Sexual differentiation of the urogenital sinus ridge. (*A*–*H*) Whole mount lacZ-stained male and female $Shh^{GFPcre/+}$; $R26R^{lacZ/+}$ embryos from E14.5–E17.5. (*I*) Graph showing the length of the urethra from the bladder to the sinus ridge and total urethral length in male and female individuals. (*J*) Schematic showing how the position of the sinus ridge was determined; the length from the bladder to the sinus ridge was divided by the total length of the urethra; the red and blue lines represent the Wolffian and Müllerian ducts. (*K*) Graph showing the position of the sinus ridge relative to the length of the urethra in male and female embryos from E14.5–E17.5. bl, bladder; sr, sinus ridge; gt, genital tubercle; p, prostate buds; and bug, bulbourethral gland. $^{**}P < 0.01$ and $^{***}P < 0.001$, using a two-tailed *t* test to compare male versus female.

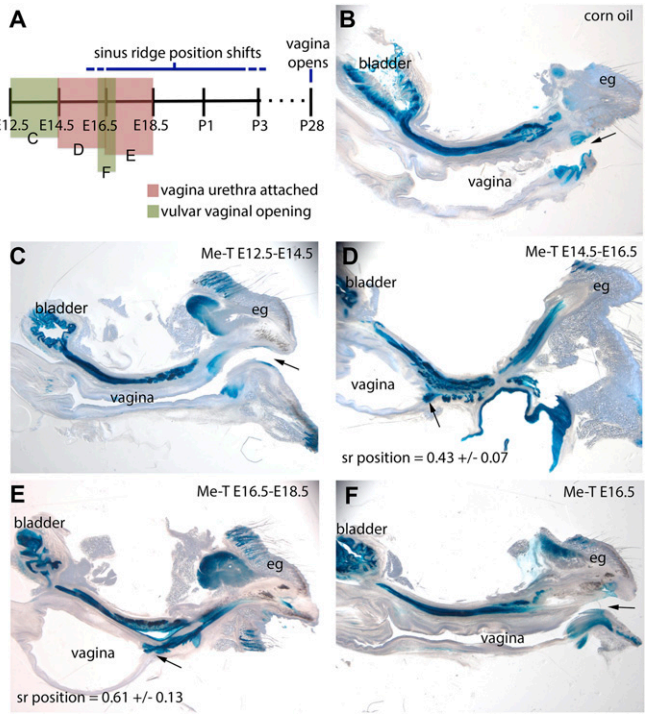

Fig. 2. Me-T treatment windows and effect on vaginal position. (*A*) Schematic showing when the position of the sinus ridge shifts and when the vagina opens; the four different Me-T treatment windows are shown. Red indicates vaginal attachment to the urethra at P28, and green indicates a vaginal opening has formed in the vulva. (*B–F*) LacZ-stained P28 female $Shh^{GFPcre/+}$; $R26R^{lacZ/+}$ vibratome sections. (*B*) Corn oil treated from E14.5–E16.5. (*C*) Me-T treated from E12.5–14.5. (*D*) Me-T treated from E14.5–E16.5; the sinus ridge position along the urethra is noted. (*E*) Me-T treated from E16.5–E18.5; the sinus ridge position along the urethra is noted. (*F*) Me-T treated at E16.5 only. eg, external genitalia. Arrows indicate the position of the sinus ridge or vaginal opening.

although the position of attachment varied between these groups (Fig. 2 *D* and *E*). The E14.5–E16.5 treatment window led to a more proximal urethrovaginal attachment on average than the E16.5–E18.5 group, although the difference between these groups was not significant (Fig. 2 *D* and *E*). By contrast, androgen treatment at E12.5–E14.5 did not cause vaginal attachment to the urethra, as the vagina was open in the vulva at P28, similar to the corn-oil–treated control females (Fig. 2 *B* and *C*). Thus, the timing of androgen exposure after E14.5 determines the position of vaginal attachment along the urethra.

Because sustained treatment with androgen during two overlapping 3-day windows disrupted formation of the vaginal opening, we next tested whether an acute exposure to androgen is sufficient to induce vaginal attachment to the urethra. When embryos were treated with a single dose of androgen at E16.5—a time point shared by both of the 3-day treatment windows that inhibited formation of a vaginal opening—females developed a normal vaginal opening in the vulva (Fig. 2*F*). Thus, acute exposure to androgen in the middle of the sensitive period is not sufficient to disrupt development of the vagina in mice.

To determine how androgen exposure affects sinus ridge morphogenesis to induce a urethrovaginal attachment, we examined urethral morphology and relative position of the sinus ridge of the E16.5, the E12.5–E14.5, and the E14.5–E16.5 Me-T treatment groups at E17.5. The E14.5–E16.5 exposure resulted in masculinization of sinus ridge position and urethral length at E17.5. Indeed, urethral morphology of these females was almost indistinguishable from control males (Fig. 3 *A–C*, *F*, and *G*). The E12.5–E14.5-treated females did not show significant masculinization of sinus ridge position or urethral morphology at E17.5 (Fig. 3 *E–G*), consistent with our finding that these mice form a vaginal opening in the vulva (Fig. 2). Surprisingly, although females exposed to Me-T at E16.5 had a vaginal opening in the vulva when examined at P28, we observed significant masculinization of the sinus ridge relative position at E17.5 (Fig. 3 *D* and *F*). However, despite the anterior position of the sinus ridge, neither urethral length nor morphology was significantly different from control females (Fig. 3*G*). Thus, acute exposure to androgen during the critical period can retard descent of the sinus ridge, but morphogenesis resumes after withdrawal of the androgenic signal. Taken together, these results indicate that both the timing and the duration of androgen exposure at fetal stages determines sinus ridge position and urethral morphology, but masculinization of sinus ridge position at fetal stages does not necessarily result in persistence of a urethrovaginal attachment at puberty.

Androgen Receptor in the Urogenital Sinus Mediates the Effects of Me-T on Sinus Ridge Morphogenesis. Although testosterone can be converted to estradiol by aromatase, Me-T is not readily aromatized and it can inhibit aromatase in some circumstances (19–21). We reasoned that the effects of Me-T on sinus ridge morphogenesis and vaginal development are mediated by AR, but it was unclear whether Me-T acts directly on sinus ridge cells or via the gonads, where it could potentially disrupt gonadal development and steroidogenesis. To distinguish between these possibilities, we administered Me-T at E14.5–E16.5 to embryos in which a floxed allele of *Ar* was conditionally deleted (Ar^{A}) from the urogenital

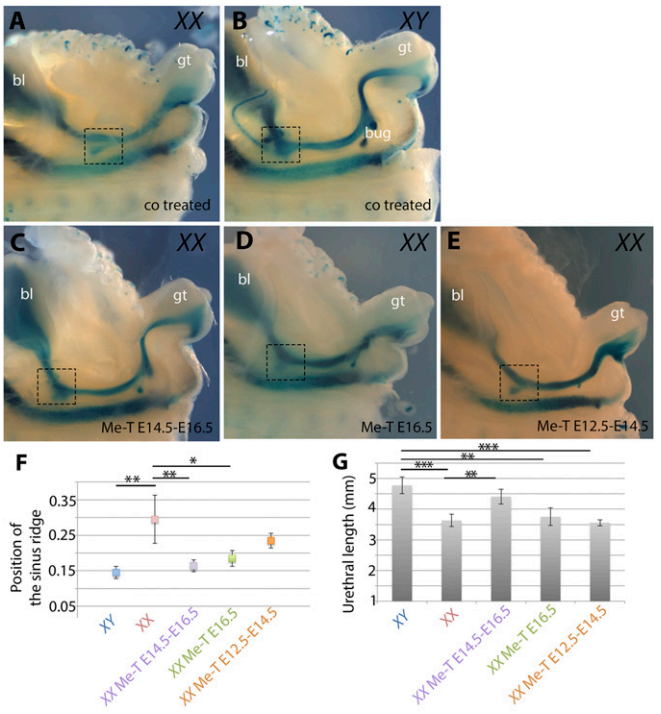

Fig. 3. Masculinization of the urethra and sinus ridge position by Me-T exposure during discrete temporal windows of fetal development. (*A–E*) Whole mount lacZ-stained E17.5 $Shh^{GFPcre/+}$; $R26R^{lacZ/+}$ embryos, lateral view. (*A* and *B*) Corn-oil–treated male and female; the sinus ridge is in the boxed region. (*C*) Me-T treated during the E14.5–E16.5 time window. (*D*) Me-T treatment at E16.5. (*E*) Me-T treated from E12.5–E14.5. (*F*) Graph showing the position of the sinus ridge at E17.5 for each treatment group relative to total urethral length. (*G*) Graph showing the total length of the urethra at E17.5 for each treatment group. bl, bladder; sr, sinus ridge; gt, genital tubercle. **P* < 0.05, ***P* < 0.01, or ****P* < 0.001, using ANOVA.

sinus using *Hoxa13*^{cre}, which is expressed in the urogenital sinus epithelium and mesenchyme but not the fetal gonads (Fig. S1). Integrin-β4 immunofluorescence to examine urogenital sinus morphology revealed that, despite Me-T treatment, the sinus ridge position was feminized in *Hoxa13*$^{cre/+}$; *Ar*$^{\Delta/\Delta}$ females and *Hoxa13*$^{cre/+}$; *Ar*$^{\Delta/Y}$ males at E17.5, whereas Me-T induced masculinization of sinus ridge (i.e., its position remained anterior/proximal) in male and female mice without *Ar* deletion (Fig. 4 *A*–*E*). These results are consistent with studies in *Ar*^{Tfm} males, which lack a functional androgen receptor, show posterior/distal movement of their sinus ridge, and have a vaginal pouch that opens in the perineum (Fig. S2) (6, 22). Taken together, these data show that androgen acts directly on AR$^+$ cells in the urogenital sinus to prevent the distal shift of sinus ridge position along the urethra.

Sexual Differentiation of the Sinus Ridge Position Is Independent of Wolffian and Müllerian Duct Development. The Wolffian and Müllerian ducts attach to the urogenital sinus at the sinus ridge, and the sex ducts themselves undergo sexual differentiation or degradation in response to hormonal cues. By E17.5, the rostral Müllerian and Wolffian ducts have degenerated in males and females, respectively (13, 23). To determine if the sinus ridge position is influenced by differential development of the male and female sex ducts, we examined Wolffian and Müllerian duct development in females treated with Me-T and in males with *Ar* deleted by *Hoxa13*^{cre}. In females exposed to Me-T from E14.5–E16.5, which masculinizes the sinus ridge (Figs. 2 and 3), Müllerian ducts were maintained but Wolffian ducts were rudimentary at E17.5 similar to control females at this stage (Fig. 5 *A*, *B*, *E*, and *F*). Reciprocally, deletion of *Ar* in the sinus ridge of male embryos (*Hoxa13*$^{cre/+}$; *Ar*$^{\Delta/Y}$), which results in feminization of the sinus ridge (Fig. 4), did not result in rudimentary Wolffian ducts at E17.5 and their morphology was similar to control males although the mutant epithelium was thinner (Fig. 5 *C*, *D*, *G*, and *H*). In both *Hoxa13*$^{cre/+}$; *Ar*$^{\Delta/Y}$ and control males, the Wolffian ducts extended to the testes and a Müllerian duct remnant was found caudally (Fig. 5 *C*, *D*, *G*, and *H*). Together, these results indicate that sexually dimorphic development of the sinus ridge is independent of sex duct morphogenesis.

Masculinization of the Sinus Ridge Is Controlled by AR in Urogenital Sinus Mesenchyme. *Ar* is expressed in the urogenital sinus mesenchyme and epithelium at E12.5, when androgen is beginning to be produced in the testes (24, 25). Having demonstrated that androgen acts directly on AR in urogenital sinus cells, rather than via the gonads, to inhibit feminization of the sinus ridge, we next asked whether the androgenic response is mediated by one or both cell types in the urogenital sinus. We conditionally deleted *Ar* in males in individual tissue compartments using cell type-specific *cre* alleles; *Shh*^{GFPcre} was used to inactivate *Ar* in urogenital sinus epithelium and *Twist2*^{cre} (formerly called *Dermo1*^{cre}) was used to delete *Ar* in urogenital sinus mesenchyme. Deletion of *Ar* in urogenital sinus epithelium (*Shh*$^{GFPcre/+}$; *Ar*$^{\Delta/Y}$) did not affect the position of the sinus ridge or the length of the urethra at E17.5 (Fig. 6 *A*–*C*, *G*, and *H*). However, when AR was removed from urogenital sinus mesenchyme (*Twist2*$^{cre/+}$; *Ar*$^{\Delta/Y}$), the sinus ridge relative position shifted distally and the urethra failed to undergo urethral elongation at E17.5 (Fig. 6 *D*–*H*). Thus, deletion of AR in mesenchymal cells of the male urogenital sinus is sufficient to initiate the first step of formation of a vaginal opening in the vulva, indicating that only mesenchymal AR is necessary to prevent sinus ridge movement and urethral masculinization.

Mosaic Analysis Reveals a Subpopulation of AR$^+$ Mesenchymal Cells That Controls Sexual Differentiation of the Sinus Ridge Position. Epithelial–mesenchymal interactions can control morphogenesis by induction of paracrine factors that signal between the epithelium and mesenchyme, by direct contact between epithelial and mesenchymal cells, or by influencing the extracellular matrix shared between these compartments (26–28). To examine how mesenchymal AR prevents movement of the sinus ridge, we took advantage of X inactivation and performed mosaic analysis of *Ar* conditional mutants. Because *Ar* is on the X chromosome, this allowed us to generate Me-T–treated females with varied amounts and localizations of AR$^+$ cells in the urogenital sinus, which resulted in an array of sinus ridge positions and urethral masculinization phenotypes (Fig. 7 *A*–*F*). By determining the spatial localization of AR$^+$ cells relative to the position of the sinus ridge, we tested whether a subpopulation of androgen-responsive mesenchymal cells regulates morphogenesis of the sinus ridge.

We generated *Hoxa13*$^{cre/+}$; *Ar*$^{\Delta/+}$ mosaic female embryos and treated them with Me-T from E14.5–E16.5. Because of X inactivation, the heterozygous floxed females carrying *cre* were expected to have both AR$^+$ and AR$^-$ cells in the urogenital sinus. Analysis of the number and positions of AR$^+$ cells in sinus ridge mesenchyme revealed that mosaic females had a disproportionate number of AR$^+$ cells immediately adjacent to the urethral epithelium (Fig. 7 *G* and *H*). We found a significant correlation ($R^2 = 0.75$, $P = 0.005$) between the number AR$^+$ mesenchymal cells in direct contact with the basement membrane and the position of the sinus ridge (Fig. 7*H*). The number of AR$^+$ cells throughout the mesenchyme

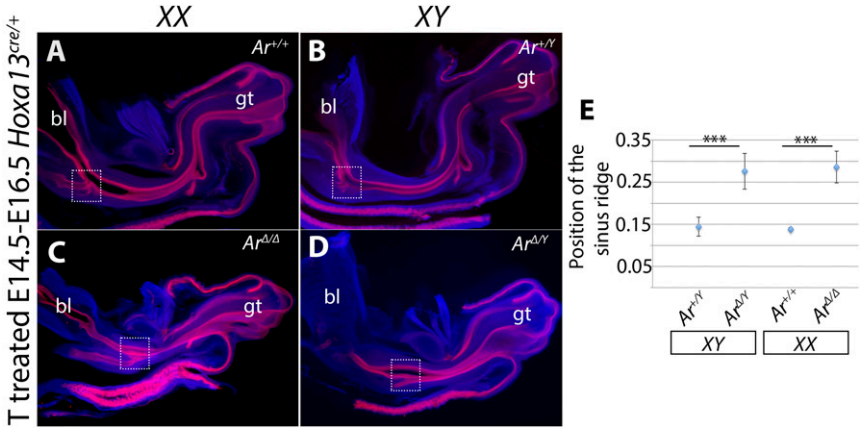

Fig. 4. Androgen acts through AR to prevent sinus ridge movement. (*A*–*D*) Vibratome sagittal sections of E17.5 embryos stained with phalloidin and integrin-β4 to mark the boundary of the urethral epithelium; the sinus ridge is in the boxed region. (*A* and *B*) Me-T–treated *Hoxa13*$^{cre/+}$ female and male embryos. (*C* and *D*) Me-T–treated female and male embryos with *Ar* deleted with *Hoxa13*^{cre}. (*E*) Graph showing the relative position of the sinus ridge control and *Ar*-deleted males and females. bl, bladder; gt, genital tubercle. ***$P < 0.001$, using ANOVA.

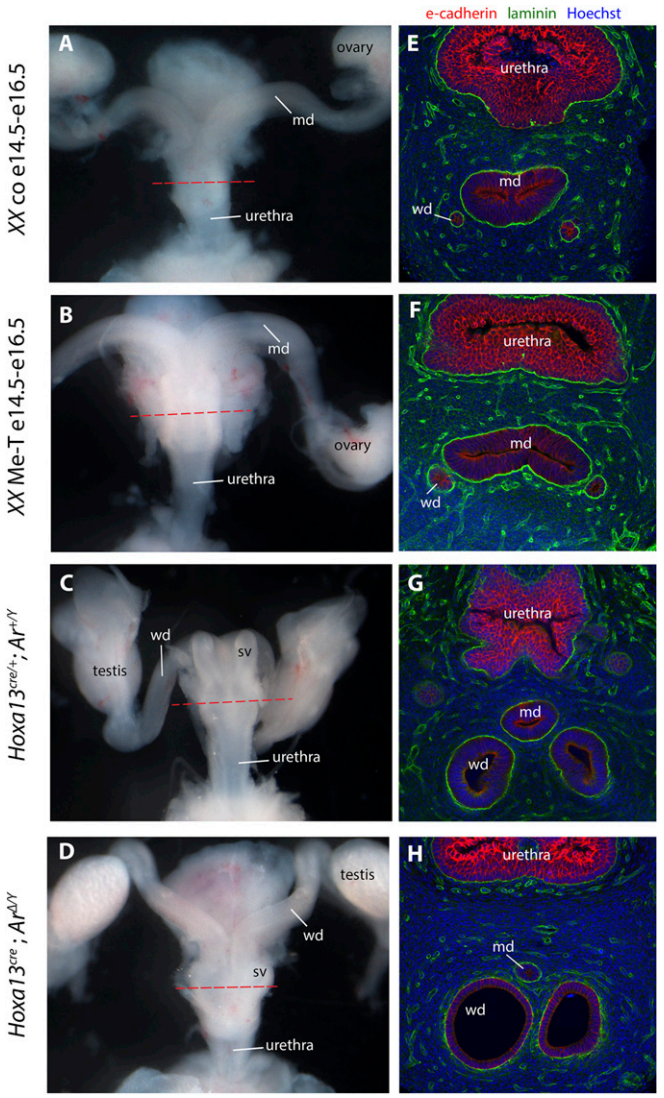

Fig. 5. Wolffian and Müllerian duct morphology after prenatal androgen treatment. (*A–D*) Whole mount images of E17.5 lower genitourinary tract of Me-T–treated (*B*) or untreated (*A*) females and *Hoxa13*$^{cre/+}$ males that are wild-type (*C*) or have *Ar* deleted (*D*); dorsal view. (*E–H*) Sections showing immunofluorescence for e-cadherin to label the Wolffian and Müllerian ducts; the plane of section in shown by the hashed red line in *A–D*; ventral is toward the *Top*. (*E* and *F*) Caudal Wolffian duct remnants are found both in control females and in females treated with Me-T. (*G* and *H*) The Wolffian ducts and caudal Müllerian duct remnants are present both in wild-type males and in males with *Ar* deleted by *Hoxa13*^{cre}. md, Müllerian duct; wd, Wolffian duct; sv, seminal vesicle.

also correlated with the position of the sinus ridge ($R^2 = 0.55$, $P = 0.04$, Fig. 7*G*), but the correlation was weaker than that obtained with cells in direct contact with the basement membrane. By contrast, there was no significant correlation between the number of AR$^+$ cells in the epithelium and position of the sinus ridge ($R^2 = 0.39$, $P = 0.09$, Fig. 7*I*), consistent with our finding that epithelial deletion of AR does not affect sinus ridge position. Taken together, these results indicate that AR signaling in the mesenchyme immediately adjacent to the urethral epithelium determines the position of the sinus ridge.

Discussion

Hormonal regulation of sexual differentiation in the lower genitourinary tract is only beginning to be understood, and cellular targets of endogenous and exogenous endocrine signals are largely unknown. Several studies have examined the sinus ridge and its contribution to formation of the vaginal opening. Foundational work from Drews et al. using organ culture and *Ar*^{Tfm} mutant mice demonstrated the requirement of androgen in inhibiting movement of the sinus ridge and suggested that mesenchymal AR signaling is likely important to prevent sinus ridge movement (6, 7, 29, 30). More recent studies showed that the dose of androgen can determine the position of the sinus ridge (8, 9, 16, 17). In this study, we examined the role of androgen in sexual differentiation of the sinus ridge position, a structure that is required for proper placement of the vaginal opening in the vulva of females and for positioning the ejaculatory duct entry site in the

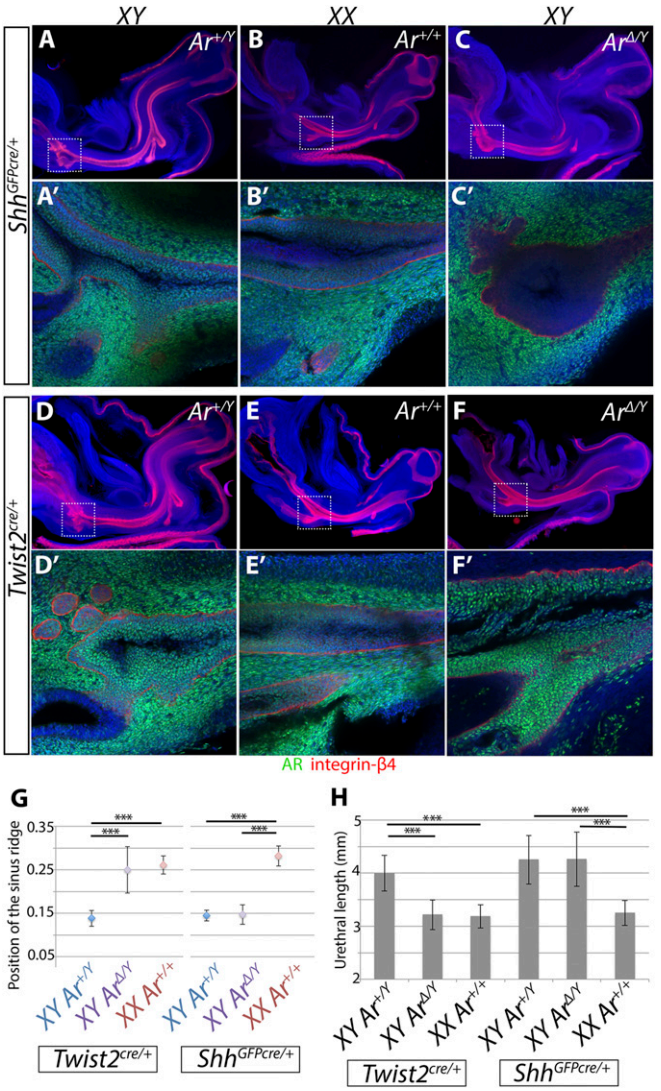

Fig. 6. Androgen receptor in urogenital sinus mesenchyme is required to prevent sinus ridge movement. (*A–F*) Vibratome sections of E17.5 embryos stained with phalloidin and integrin-β4 to mark the boundary of the urethral epithelium. (*A–C*) Wild-type male (*A*), female (*B*), and *Shh*$^{GFPcre/+}$; *Ar*$^{\Delta/Y}$ male (*C*). (*A′–C′*) Higher magnification of the boxed region showing immunofluorescence for AR. (*C′*) AR staining is lost in the epithelium. (*D–F*) male (*D*), female (*E*), and *Twist2*$^{cre/+}$; *Ar*$^{\Delta/Y}$ male (*F*). (*D′–F′*) Higher magnification of the boxed region showing immunofluorescence for AR. (*F′*) AR staining is lost in the mesenchyme. (*G*) Graph showing the position of the sinus ridge relative to urethral length in the *Twist2*^{cre} and *Shh*^{GFPcre} deletions of *Ar*. (*H*) Urethral length in *Twist2*^{cre} (mesenchymal) and *Shh*^{GFPcre} (epithelial) deletions of AR. gt, genital tubercle. ***$P < 0.001$, using ANOVA.

urethra of males. The results show that development of the vaginal orifice in the external genitalia and feminization of the urethra are coordinated by a population of mesenchymal cells that orchestrate descent of the sinus ridge, and that activation of AR in these cells during a defined period of prenatal development can produce the suite of structural defects found in females with CAH.

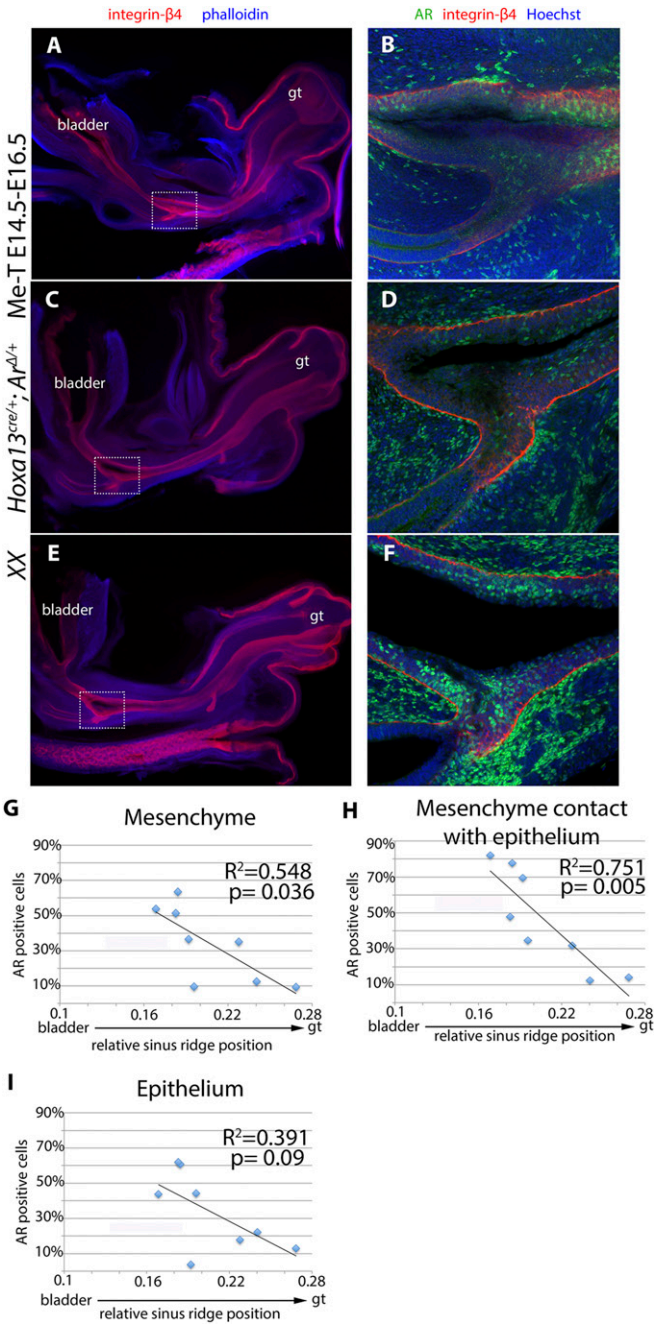

Fig. 7. Mosaic analysis of androgen signaling in Me-T–treated females. (*A*, *C*, and *E*) Vibratome sections of three representative E17.5 *Hoxa13*$^{cre/+}$; *Ar*$^{\Delta/+}$ samples with varying degrees of masculinization; samples are stained with phalloidin and integrin-β4 to outline the urethral epithelium. (*B*, *D*, and *F*) Immunofluorescence for AR and integrin-β4 shows the extent of mosaicism in the urogenital sinus mesenchyme and epithelium. *B*, *D*, and *F* correspond to the boxed regions in *A*, *C*, and *E*. (*G*–*I*) Graphs showing the correlation between AR$^+$ cells and position of the sinus ridge in the mesenchyme (*G*), in the mesenchyme cells in contact with the basement membrane of the epithelium (*H*) and in the epithelium alone (*I*). gt, genital tubercle.

Timing and Duration of Androgen Signaling Influences Development of the Vaginal Opening. Establishing the critical developmental time period when the sinus ridge is responsive to the influence of hormones is crucial for understanding not only how sinus ridge morphogenesis leads to formation of the vagina, but also how its development is perturbed by exposure to endocrine disruptors and by genetic DSDs. We found that the timing and duration of androgen exposure can determine the site of vaginal attachment to the urethra. We showed that androgen exposure during a 3-day period of development, when the sinus ridge position shifts toward the perineum, is sufficient to cause vaginal attachment to the urethra and to prevent vaginal opening in the vulva, with the most proximal confluence resulting from disruption during E14.5–E16.5 in mice. This temporal window coincides with the stage when sexual differentiation becomes apparent in the urogenital sinus of males and females and overlaps with the critical period when androgen signaling was found to be important for sexual differentiation of the urethra in the phallus of male mice (31, 32). Taken together, these results indicate that endocrine signaling during a short time window, from E14.5 to E16.5, is critical for masculinization or feminization of the lower urogenital tract.

We found that the duration of androgen signaling during this critical period determines whether the vagina attaches to the urethra or opens in the vulva. A single day of androgen exposure during the same critical period disrupted sinus ridge movement, but did not cause the vagina to remain attached to the urethra at puberty. Given that this transient exposure did not cause a significant difference in urethral length or masculinization of the urethra, we posit that the ability of the sinus ridge to reach the perineum and allow formation of the vaginal opening is due to the relatively mild masculinization of urethra as a whole. In support of this hypothesis, Me-T–treated females that maintained vaginal–urethral attachment had significantly longer urethrae at E17.5 (E14.5–E16.5 treatment group) compared with Me-T–treated females that developed vaginal openings in the vulva (both E12.5–E14.5 and single day treatment groups). These results support a model in which differential urethral growth is responsible for the relative shift in sinus ridge position in females, such that lengthening and masculinization of the urethra by increased androgen exposure would prevent the sinus ridge from reaching the perineum in androgen-exposed females (33, 34).

Androgen Signaling in Mesenchyme Adjacent to the Urethra Regulates Sinus Ridge Position. Although the androgen receptor is expressed in both the epithelium and mesenchyme of the urogenital sinus, mesenchymal androgen signaling alone regulates sinus ridge position. This is similar to the indirect mode of androgen action on other epithelial structures, such as the mammary gland, prostate, and phallic urethra (31, 35–40).

Signaling between epithelial and mesenchymal compartments is critical to the development of many epithelial tissues, including the urogenital tract. The urogenital sinus mesenchyme has several different subcompartments, including the lamina propria immediately beneath the epithelium, the submucosal mesenchyme, and the developing muscle. Mesenchymal pads are found near the outer developing muscular layer and are required for inducing prostate budding, although these mesenchymal domains are not in direct contact with the epithelium (41, 42). Prostate induction requires paracrine signaling from the mesenchymal pad, and secreted factors such as FGF10 have been shown to be required for this induction (42, 43). Our mosaic analysis demonstrates that AR$^+$ cells in the mesenchyme exhibit a biased pattern of localization near the basement membrane of the urethra, similar to the patterns described in the developing mammary gland and prostate (44, 45). Our results suggest that AR$^+$ mesenchymal cells in contact with the basement membrane have functional significance, as the number of AR$^+$ cells within this lamina propria domain correlated significantly with the position of the sinus ridge. This

subdomain of mesenchymal cells within the lamina propria may therefore act as an androgen-mediated signaling center to control sexual differentiation of the sinus ridge and the urethra, which suggests that AR^+ cells may act in a juxtacrine manner or via the basement membrane to regulate sinus ridge epithelial morphogenesis. Such basement membrane-mediated interactions have been identified in mammary gland, tooth, and gut development, where direct epithelial–mesenchymal contact is required for normal epithelial morphogenesis due to influence on the basement membrane (28, 46–48). Alternatively, paracrine signaling may be responsible for determining the position of the sinus ridge, either independently or in conjunction with signaling to the basement membrane or to the epithelium through direct contact. Defining AR targets in the urogenital sinus mesenchyme will be an important next step for determining how androgen affects morphogenesis of the sinus ridge.

Sexual Dimorphism of the Sinus Ridge Position and Urethral Morphogenesis in Females. A better understanding of how sinus ridge position changes during development has broader implications for our understanding of urogenital sinus development and sexual differentiation. There are several possibilities to explain sinus ridge movement. The sinus ridge may move by (*i*) differential growth of the urethra anterior and posterior to the sinus ridge, (*ii*) collective cell migration of the sinus ridge cells, or (*iii*) septation of the sinus ridge from the urethra in a rostral-to-caudal direction. Surprisingly little is known about the development of several components of the female reproductive tract, such as the hymen, Bartholin's gland, and Skene's gland (49). The Skene's gland in females has long been referred to as the homolog of the male prostate; however, the Skene's gland is positioned at the urethral orifice in females, which contrasts with the position of the prostate in the pelvic urethra in males (50, 51). We predict that the shift in sinus ridge position occurs as a result of differential growth of the urethra, whereby the urethra anterior to the sinus ridge grows more rapidly or for a longer period than the posterior urethra in females, which would displace the sinus ridge posteriorly. This would also explain the position of the Skene's gland near the urethral opening of adult females. In support of this hypothesis, it has been suggested that in human fetuses, the entire female urethra is equivalent to the male prostatic urethra, although further comparisons of cell type identities between male and female urethrae are needed (33).

In summary, our results show how androgen influences sexual differentiation of the urethra and movement of the sinus ridge, processes that are important for formation of the vaginal opening in the external genitalia of females. These findings provide a framework for future studies of sexual differentiation of the urogenital sinus, movement of the sinus ridge, and the role of androgen signaling, and provide a foundation for understanding development of the vaginal opening and the mechanisms underlying lower genitourinary tract defects in DSDs.

Materials and Methods

Mice and Me-T Treatment. The $Ar^{tm1Verh}$ mouse line (abbreviated Ar^{Δ} after cre excision) was provided by Guido Verhoeven, Katholieke Universiteit Leuven, Belgium, via Marvin Maestrich and Connie Wang, University of Texas M. D. Anderson Cancer Center, Houston. The $Hoxa13^{tm1(cre)Makm}$ mouse line (abbreviated $Hoxa13^{cre}$) was provided by Marie Kmita, Institut de Recherches Cliniques de Montreal, Montreal. The $Shh^{tm1(EGFP/cre)Cjt}$ mouse line (abbreviated Shh^{GFPcre}) was provided by Brian Harfe, University of Florida, Gainesville, FL. $Twist2^{tm1.1(cre)Dor}$ (abbreviated $Twist2^{cre}$), $Gt(Rosa)26Sor^{tm1Sor}$ (abbreviated $R26R^{lacZ}$), and Ar^{Tfm} mice were purchased from The Jackson Laboratory.

CD1 female mice (Envigo) were crossed to $Shh^{GFPcre/+}$ males for examination of sinus ridge morphology and for androgen exposure time windows. The 17α-Me-T (Sigma, M7252) was dissolved to 100 mg/mL in ethanol before diluting to 4.8 mg/mL in filtered, tocopherol-stripped corn oil. A dosage of 12 mg/kg was administered by gavage to pregnant females once daily at E12.5–E14.5, E14.5–E16.5, E16.5–E18.5, or E16.5 alone. Control mice of the same genotype were administered ethanol diluted in filtered, tocopherol-stripped corn oil. All treatments were repeated with at least three litters and ANOVA was performed on averages from each litter. For genetic experiments or comparisons of wild-type males and females, ANOVA or *t* tests were performed on at least four individuals from at least three litters. All experiments were performed in accordance with the University of Florida Institutional Animal Care and Use Committee Protocol 201203399.

Immunofluorescence and Mosaic Analysis. Embryos were dissected, fixed in 4% (wt/vol) paraformaldehyde (PFA) for 1 h, washed in PBS for 2 h, and then embedded in 6% (wt/vol) low-melt agarose. The embryos were vibratomed at 150 μm. Immunofluorescence was then performed in 2-mL tubes by blocking for 1 h in 0.1% Triton X-100, 1% goat serum in PBS. Primary antibodies against AR (Santa Cruz, sc-816; diluted 1:50) and integrin-β4 (Abcam, ab25254; 1:500) were incubated overnight at 4 °C. After a series of washes in 0.1% Triton X-100, 1% goat serum in PBS, secondary antibodies [goat anti-rabbit Alexa 647 (Life Technologies, A-21245; 1:300) and goat anti-rat Cy3 (Jackson ImmunoResearch Labs, 112–165-167; 1:300)], phalloidin 488 (Life Technologies, A12379; 1:40), and Hoechst (Invitrogen, 1:3,000) were incubated with the sections overnight at 4 °C. The sections were visualized using a dissecting microscope at 2.5× to determine urethral morphology followed by a Zeiss LSM 710 confocal microscope to visualize AR staining. The percentage of AR^+ cells was determined by counting the number of AR^+ cells relative to the number of Hoechst-stained nuclei at 63× in the dorsal urethra: one image was counted just anterior to and including part of the sinus ridge and one image just posterior to and including part of the sinus ridge. Nuclei were counted using the ImageJ multipoint tool.

LacZ Staining. X-gal staining of embryos, pups, and adults were carried out as follows. The lower genitourinary tract was dissected away and the tissue was fixed in 4% (wt/vol) PFA for 1 h. The tissue was then washed three times in lacZ buffer (0.1 M pH 7.4 NaPhosphate, 1% NaDeoxycholate, 2 mM $MgCl_2$, 0.2% IGEPAL CA-630), and stained overnight at room temperature in staining solution [1 mg/mL X-gal, 0.5 mM $K_3[Fe(Cn)_6]$, 5 mM $K_4[Fe(Cn)_6]$ in lacZ buffer]. After staining, the lower genitourinary tract was imaged in whole mount (fetal stages) or embedded in 6% (wt/vol) low-melt agarose and vibratomed at 150 μm (P28).

ACKNOWLEDGMENTS. We thank G. Verhoeven, M. Maestrich, C. Wang, M. Kmita, and B. Harfe for providing mice and B. Armfield, K. Lewis, R. Rajakumar, M. Gredler, and other members of the M.J.C. laboratory for comments on the manuscript. This work was supported by NIH/National Institute of Diabetes and Digestive and Kidney Diseases Grant K01 DK105077 (to C.E.L.) and NIH/National Institute of Environmental Health Sciences Grant R01 ES017099 (to M.J.C.).

1. Hutson JM, Grover SR, O'Connell M, Pennell SD (2014) Malformation syndromes associated with disorders of sex development. *Nat Rev Endocrinol* 10(8):476–487.
2. Ono M, Harley VR (2013) Disorders of sex development: New genes, new concepts. *Nat Rev Endocrinol* 9(2):79–91.
3. Lee PA, Houk CP, Ahmed SF, Hughes IA; International Consensus Conference on Intersex organized by the Lawson Wilkins Pediatric Endocrine Society and the European Society for Paediatric Endocrinology (2006) Consensus statement on management of intersex disorders. *Pediatrics* 118(2):e488–e500.
4. Hutson JM, Warne GL, Grover SR (2012) *Disorders of Sex Development* (Springer, New York).
5. Rawal AY, Austin PF (2015) Concepts and updates in the evaluation and diagnosis of common disorders of sexual development. *Curr Urol Rep* 16(12):83.
6. Drews U, Sulak O, Schenck PA (2002) Androgens and the development of the vagina. *Biol Reprod* 67(4):1353–1359.
7. Drews U (2007) Helper function of the Wolffian ducts and role of androgens in the development of the vagina. *Sex Dev* 1(2):100–110.
8. Yucel S, Cavalcanti AG, Wang Z, Baskin LS (2003) The impact of prenatal androgens on vaginal and urogenital sinus development in the female mouse. *J Urol* 170(4 Pt 1):1432–1436.
9. Wolf CJ, Hotchkiss A, Ostby JS, LeBlanc GA, Gray LE, Jr (2002) Effects of prenatal testosterone propionate on the sexual development of male and female rats: A dose-response study. *Toxicol Sci* 65(1):71–86.
10. Georgas KM, et al. (2015) An illustrated anatomical ontology of the developing mouse lower urogenital tract. *Development* 142(10):1893–1908.
11. Dyche WJ (1979) A comparative study of the differentiation and involution of the Mullerian duct and Wolffian duct in the male and female fetal mouse. *J Morphol* 162(2):175–209.
12. Koff AK (1933) Development of the vagina in the human fetus. *Contrib Embryol* 24(140):59–91.
13. Orvis GD, Behringer RR (2007) Cellular mechanisms of Müllerian duct formation in the mouse. *Dev Biol* 306(2):493–504.
14. Kurita T (2010) Developmental origin of vaginal epithelium. *Differentiation* 80(2–3):99–105.
15. Rodriguez I, Araki K, Khatib K, Martinou JC, Vassalli P (1997) Mouse vaginal opening is an apoptosis-dependent process which can be prevented by the overexpression of Bcl2. *Dev Biol* 184(1):115–121.

16. Hotchkiss AK, Furr J, Makynen EA, Ankley GT, Gray LE, Jr (2007) In utero exposure to the environmental androgen trenbolone masculinizes female Sprague-Dawley rats. *Toxicol Lett* 174(1–3):31–41.
17. Hotchkiss AK, et al. (2007) Prenatal testosterone exposure permanently masculinizes anogenital distance, nipple development, and reproductive tract morphology in female Sprague-Dawley rats. *Toxicol Sci* 96(2):335–345.
18. Grumbach MM, Ducharme JR (1960) The effects of androgens on fetal sexual development: Androgen-induced female pseudohermaphrodism. *Fertil Steril* 11:157–180.
19. Mor G, et al. (2001) 17alpha-methyl testosterone is a competitive inhibitor of aromatase activity in Jar choriocarcinoma cells and macrophage-like THP-1 cells in culture. *J Steroid Biochem Mol Biol* 79(1–5):239–246.
20. Attardi BJ, et al. (2008) Dimethandrolone (7alpha,11beta-dimethyl-19-nortestosterone) and 11beta-methyl-19-nortestosterone are not converted to aromatic A-ring products in the presence of recombinant human aromatase. *J Steroid Biochem Mol Biol* 110(3-5):214–222.
21. Fisher CR, Graves KH, Parlow AF, Simpson ER (1998) Characterization of mice deficient in aromatase (ArKO) because of targeted disruption of the cyp19 gene. *Proc Natl Acad Sci USA* 95(12):6965–6970.
22. Schleicher G, Stumpf WE, Thiedemann KU, Drews U (1988) Intersex mice composed of androgen insensitive Tfm and wild-type cells analysed by 3H dihydrotestosterone autoradiography. *Anat Embryol (Berl)* 178(6):521–528.
23. Welsh M, Sharpe RM, Walker M, Smith LB, Saunders PT (2009) New insights into the role of androgens in wolffian duct stabilization in male and female rodents. *Endocrinology* 150(5):2472–2480.
24. Crocoll A, Zhu CC, Cato AC, Blum M (1998) Expression of androgen receptor mRNA during mouse embryogenesis. *Mech Dev* 72(1–2):175–178.
25. Cooke PS, Young P, Cunha GR (1991) Androgen receptor expression in developing male reproductive organs. *Endocrinology* 128(6):2867–2873.
26. Jerman UD, Kreft ME, Veranič P (2015) Epithelial-mesenchymal interactions in urinary bladder and small intestine and how to apply them in tissue engineering. *Tissue Eng Part B Rev* 21(6):521–530.
27. Donjacour AA, Cunha GR (1991) Stromal regulation of epithelial function. *Cancer Treat Res* 53:335–364.
28. Bonnans C, Chou J, Werb Z (2014) Remodelling the extracellular matrix in development and disease. *Nat Rev Mol Cell Biol* 15(12):786–801.
29. Drews U, Schleicher G, Stumpf WE, Thiedemann KU (1988) Androgen receptor-deficient Tfm cells in the mosaic epididymis of sex-reversed mice heterozygous for Tfm: An autoradiographic study with [3H]-dihydrotestosterone and [^{3}H]-estradiol. *Anat Rec* 220(4):393–396.
30. Drews U, Sulak O, Oppitz M (2001) Immunohistochemical localisation of androgen receptor during sex-specific morphogenesis in the fetal mouse. *Histochem Cell Biol* 116(5):427–439.
31. Zheng Z, Armfield BA, Cohn MJ (2015) Timing of androgen receptor disruption and estrogen exposure underlies a spectrum of congenital penile anomalies. *Proc Natl Acad Sci USA* 112(52):E7194–E7203.
32. Miyagawa S, et al. (2009) Genetic interactions of the androgen and Wnt/beta-catenin pathways for the masculinization of external genitalia. *Mol Endocrinol* 23(6):871–880.
33. Masumoto H, Rodríguez-Vázquez JF, Verdugo-López S, Murakami G, Matsubara A (2011) Fetal topographical anatomy of the female urethra and descending vagina: A histological study of the early human fetal urethra. *Ann Anat* 193(6):500–508.
34. Shapiro E, Huang HY, Wu XR (2000) Uroplakin and androgen receptor expression in the human fetal genital tract: Insights into the development of the vagina. *J Urol* 164(3 Pt 2):1048–1051.
35. Yu S, et al. (2012) Altered prostate epithelial development in mice lacking the androgen receptor in stromal fibroblasts. *Prostate* 72(4):437–449.
36. Cunha GR (1972) Tissue interactions between epithelium and mesenchyme of urogenital and integumental origin. *Anat Rec* 172(3):529–541.
37. Cunha GR, Donjacour AA (1989) Mesenchymal-epithelial interactions in the growth and development of the prostate. *Cancer Treat Res* 46:159–175.
38. Donjacour AA, Cunha GR (1993) Assessment of prostatic protein secretion in tissue recombinants made of urogenital sinus mesenchyme and urothelium from normal or androgen-insensitive mice. *Endocrinology* 132(6):2342–2350.
39. Ipulan LA, et al. (2016) Investigation of sexual dimorphisms through mouse models and hormone/hormone-disruptor treatments. *Differentiation* 91(4–5):78–89.
40. Murashima A, Kishigami S, Thomson A, Yamada G (2015) Androgens and mammalian male reproductive tract development. *Biochim Biophys Acta* 1849(2):163–170.
41. Thomson AA, Timms BG, Barton L, Cunha GR, Grace OC (2002) The role of smooth muscle in regulating prostatic induction. *Development* 129(8):1905–1912.
42. Prins GS, Putz O (2008) Molecular signaling pathways that regulate prostate gland development. *Differentiation* 76(6):641–659.
43. Donjacour AA, Thomson AA, Cunha GR (2003) FGF-10 plays an essential role in the growth of the fetal prostate. *Dev Biol* 261(1):39–54.
44. Takeda H, Suzuki M, Lasnitzki I, Mizuno T (1987) Visualization of X-chromosome inactivation mosaicism of Tfm gene in XTfm/X+ heterozygous female mice. *J Endocrinol* 114(1):125–129.
45. Takeda H, Lasnitzki I, Mizuno T (1987) Change of mosaic pattern by androgens during prostatic bud formation in XTfm/X+ heterozygous female mice. *J Endocrinol* 114(1):131–137.
46. Haslam SZ (1986) Mammary fibroblast influence on normal mouse mammary epithelial cell responses to estrogen in vitro. *Cancer Res* 46(1):310–316.
47. Vainio S, Jalkanen M, Thesleff I (1989) Syndecan and tenascin expression is induced by epithelial-mesenchymal interactions in embryonic tooth mesenchyme. *J Cell Biol* 108(5):1945–1953.
48. Simon-Assmann P, Bouziges F, Arnold C, Haffen K, Kedinger M (1988) Epithelial-mesenchymal interactions in the production of basement membrane components in the gut. *Development* 102(2):339–347.
49. Kimberley N, Hutson JM, Southwell BR, Grover SR (2012) Vaginal agenesis, the hymen, and associated anomalies. *J Pediatr Adolesc Gynecol* 25(1):54–58.
50. Wernert N, et al. (1992) The 'female prostate': Location, morphology, immunohistochemical characteristics and significance. *Eur Urol* 22(1):64–69.
51. Tepper SL, Jagirdar J, Heath D, Geller SA (1984) Homology between the female paraurethral (Skene's) glands and the prostate. Immunohistochemical demonstration. *Arch Pathol Lab Med* 108(5):423–425.